

Psychrophily is associated with differential energy partitioning, photosystem stoichiometry and polypeptide phosphorylation in *Chlamydomonas raudensis*

Beth Szyszka, Alexander G. Ivanov, Norman P.A. Hüner*

Department of Biology and The Biotron, University of Western Ontario, 1151 Richmond St. N., London, Ontario, Canada N6A 5B7

Received 29 September 2006; received in revised form 23 November 2006; accepted 3 December 2006

Available online 9 December 2006

Abstract

Chlamydomonas raudensis UWO 241 and SAG 49.72 represent the psychrophilic and mesophilic strains of this green algal species. This novel discovery was exploited to assess the role of psychrophily in photoacclimation to growth temperature and growth irradiance. At their optimal growth temperatures of 8 °C and 28 °C respectively, UWO 241 and SAG 49.72 maintained comparable photostasis, that is energy balance, as measured by PSII excitation pressure. Although UWO 241 exhibited higher excitation pressure, measured as 1-qL, at all growth light intensities, the relative changes in 1-qL were similar to that of SAG 49.72 in response to growth light. In response to suboptimal temperatures and increased growth irradiance, SAG 49.72 favoured energy partitioning of excess excitation energy through inducible, down regulatory processes (Φ_{NPQ}) associated with the xanthophyll cycle and antenna quenching, while UWO 241 favoured xanthophyll cycle-independent energy partitioning through constitutive processes involved in energy dissipation (Φ_{NO}). In contrast to SAG 49.72, an elevation in growth temperature induced an increase in PSI/PSII stoichiometry in UWO 241. Furthermore, SAG 49.72 showed typical threonine-phosphorylation of LHCII, whereas UWO 241 exhibited phosphorylation of polypeptides of comparable molecular mass to PSI reaction centres but the absence of LHCII phosphorylation. Thus, although both strains maintain an energy balance irrespective of their differences in optimal growth temperatures, the mechanisms used to maintain photostasis were distinct. We conclude that psychrophily in *C. raudensis* is complex and appears to involve differential energy partitioning, photosystem stoichiometry and polypeptide phosphorylation.

© 2007 Elsevier B.V. All rights reserved.

Keywords: *Chlamydomonas raudensis*; Chlorophyll fluorescence; Cold acclimation; Energy partitioning; Photostasis; Psychrophily

1. Introduction

Chlamydomonas raudensis Ettl. (UWO 241) was isolated from the lowest trophic zone of Antarctica's permanently ice-covered Lake Bonney [1]. This environment is characterized by irradiance levels that do not exceed 50 $\mu\text{mol photons m}^{-2} \text{s}^{-1}$,

temperatures ranging from 4 °C to 6 °C and a narrow spectral distribution enriched in the blue-green region [2]. Therefore, this unique green alga has adapted to extremely stable conditions of low light and low temperature.

Recently, UWO 241 was identified as a psychrophilic strain of *C. raudensis* Ettl. (SAG 49.72), a mesophile which originates from a meadow pool near Rudná, Nordmähren, Czech Republic [3]. Psychrophiles ("cold-loving") are organisms which exhibit optimal growth temperatures below 15 °C but are unable to grow at temperatures above 20 °C [5]. In contrast, mesophiles exhibit the capacity to grow at both high and low temperatures but exhibit optimal growth temperatures in the range of 25° to 30 °C [5]. Previous comparative studies of *C. raudensis* UWO 241 were performed using the model mesophile, *Chlamydomonas reinhardtii*, a different *Chlamydomonas* algal species.

Abbreviations: F_o and F_m , fluorescence intensity measured when all photosystem II reaction centers are open or closed, respectively; F_s , steady-state fluorescence; LHCII, light-harvesting complex II; Φ_{NO} , constitutive processes involved in energy dissipation; Φ_{NPQ} , yield of zeaxanthin-dependent non-photochemical dissipation; PQ, plastoquinone; Φ_{PSII} , yield of photochemistry; Q_A , first stable quinone electron acceptor of photosystem II; qL, relative reduction state of Q_A

* Corresponding author. Tel.: +1 519 661 2111x86488; fax: +1 519 661 3935.

E-mail address: nhuner@uwo.ca (N.P.A. Hüner).

We are unaware of any other published examples whereby a single species exhibits both a mesophilic and psychrophilic strain. Thus, this report represents the first comparison of a mesophilic and a psychrophilic form of *Chlamydomonas raudensis*.

Regardless of the environment in which they exist, photosynthetic organisms must maintain a balance between energy input through photochemistry and subsequent energy use through metabolism and growth. This balance in cellular energy budget is called photostasis [4]. Although the regulatory mechanisms controlling photostasis are not known in detail, there is compelling evidence that photostasis is under redox control [7]. Absorption of light energy is a temperature-independent process which must be tightly coordinated with the temperature-dependent formation of ATP and NADPH and their subsequent utilization [5]. Thus, the potential for an energy imbalance is increased under conditions of either high light or cold temperatures, which lead to increased PSII excitation pressure [6]. PSII excitation pressure can be estimated by the chlorophyll fluorescence parameter 1-qL, which measures the relative reduction state of Q_A , the first stable quinone electron acceptor of PSII which, in turn, reflects the redox state of the plastoquinone pool and the intersystem electron transport chain [6,8,9].

In an attempt to compensate for exposure to high PSII excitation pressure, photosynthetic organisms respond with an array of short-term and long-term acclimatory mechanisms. On a time scale of minutes, organisms can reduce the efficiency of energy transfer to PSII either by redistributing light energy to PSI at the expense of PSII through state transitions or by dissipating excess energy as heat by non-photochemical quenching associated with the LHC (light-harvesting complex) antenna [6]. Alternatively, it has also been proposed that quenching of excess energy may occur at the reaction centers, in addition to zeaxanthin-dependent antenna quenching [10–13]. Long-term acclimatory responses include alterations in light-harvesting antenna size and adjustments of PSI : PSII stoichiometry in an attempt to balance the excitation light energy absorbed by the two photosystems [14,15].

Adaptation of *C. raudensis* UWO 241 to its unique natural environment has resulted in distinct photosynthetic features. Previous studies have shown that this Antarctic psychrophile exhibits a low chlorophyll a/b ratio (~ 2.0) that reflects low levels of PSI and PSI-associated proteins relative to PSII [16]. It has also been demonstrated that UWO 241 is a natural variant of state transitions, which is locked in state I [17]. Upon phosphorylation of the major LHCII polypeptides by a membrane bound protein kinase, state transitions involve the reversible transfer of a fraction of the PSII outer antenna to PSI [18]. Interestingly, Morgan-Kiss et al. [19] have shown that during acclimation to various light quality conditions, *C. raudensis* UWO 241 exhibits distinct phosphorylation profiles as compared to *C. reinhardtii*. Regardless of light quality, UWO 241 does not phosphorylate LHCII and other PSII-associated polypeptides, but rather phosphorylates a family of high molecular mass polypeptides (115 kDa) on threonine residues [19].

Short-term state transitions and long-term adjustments in photosystem stoichiometry operate with a common function, which is to increase the efficiency of the rate-limiting photosystem [20–23]. Although they occur at different time scales, the activation of both of these mechanisms is believed to be controlled by the same sensing component; the redox state of the PQ pool [23,24]. However, although *C. raudensis* UWO 241 does not have the capacity to perform a state transition response, this psychrophile is able to adjust photosystem stoichiometry in response to light quality [19]. This suggests that the long-term redistribution of absorbed excitation energy can function independently from the short-term state transition response [24].

Adjustments in PSII:PSI stoichiometry is thought to represent a mechanism for maintaining maximum efficiency of photosynthetic electron transport during long-term acclimation to light intensity [25,26] and light quality [27]. Under blue light, PSII is preferentially excited and the intersystem electron transport components are mostly reduced, whereas under conditions enriched in far-red light absorbed mainly by PSI, the components of the intersystem electron pool are mostly in an oxidized state [19]. In its oxidized state, the PQ pool inhibits the expression of PsaA and PsaB and in its reduced state the PQ pool activates expression of these PSI genes [28]. Light quality studies with *C. raudensis* UWO 241 have shown that this psychrophilic strain is unable to grow under red light illumination exclusively. However, when UWO 241 cultures were shifted to red light, acclimation was correlated with a decrease in PSI levels and a 4-fold increase in excitation pressure [19]. This suggests that the PQ pool is not the sensor for regulation of photosystem stoichiometry in UWO 241, and that this psychrophilic strain has a limited capacity to acclimate to red light [19].

Since this Antarctic strain of *Chlamydomonas raudensis* has adapted to a combination of low irradiance and low temperatures, to what extent has UWO 241 retained the ability to photoacclimate to varying growth temperature and growth irradiance? Given the unique photosynthetic characteristics of UWO 241 and the distinct environments to which the two *Chlamydomonas raudensis* species have adapted, we compared the capacity of UWO 241 and SAG 49.72 to maintain photostasis during long-term steady-state growth under various temperature and light regimes. In addition, we examined possible mechanisms employed by these two strains to compensate for energy imbalances by monitoring PSII energy partitioning, thylakoid polypeptide stoichiometry and pigment composition.

2. Materials and methods

2.1. Growth conditions

C. raudensis SAG 49.72 was grown axenically in Bold's basal medium (BBM) as reported previously [3] whereas *C. raudensis* UWO 241 was grown in BBM supplemented with 0.7 M NaCl. All cultures were aerated continuously under ambient CO₂ conditions in 250 mL glass Pyrex tubes suspended in temperature-regulated aquaria. Growth irradiance was generated by fluorescent tubes (Sylvania CW-40), which was measured from the center of the growth tubes with a

quantum sensor attached to a radiometer (Model LI-189; Li-Cor, Lincoln, Neb., USA). For the growth temperature experiments, cells were grown under steady state temperatures of 8° to 16 °C for UWO 241 and at 11° to 28 °C for SAG 49.72 under an irradiance of 150 $\mu\text{mol photons m}^{-2} \text{ s}^{-1}$. For the growth irradiance experiments, cells were grown at light intensities of 30 to 500 $\mu\text{mol photons m}^{-2} \text{ s}^{-1}$. In this case, cells of *C. raudensis* were grown at their optimal growth temperatures of 8 °C and 28 °C for SAG 49.72 and UWO 241 strains, respectively. Mid log phase cells were used in all experiments.

Exponential growth rates were calculated from growth curves created by monitoring chlorophyll concentration over time. For chlorophyll determination, cells were extracted with 90% acetone essentially as described in [17] and Chl content was measured as in [29].

2.2. SDS-PAGE and immunoblotting

Thylakoids were isolated as described in [19]. Thylakoid preparations from both strains of *C. raudensis* were solubilized in a 60 mM Tris (pH 7.8) buffer containing 1 mM EDTA, 12% (w/v) sucrose and 2% (w/v) SDS to attain an SDS:Chl ratio of 20:1. Samples were loaded on an equal Chl basis and not heated prior to electrophoresis. Electrophoretic separation was performed using a Mini-Protein II apparatus (Bio-Rad) with a 15% (w/v) polyacrylamide resolving gel containing 6 M Urea, 0.66 M Tris (pH 8.8) and a 8% (w/v) polyacrylamide stacking gel containing 0.125 M Tris (pH 6.8) using the Laemmli buffer system [30].

Thylakoid polypeptides separated by SDS-PAGE were transferred electrophoretically to nitrocellulose membranes (Bio-Rad, 0.2 μm pore size) at 5 °C for 1 h at 100 V. The membranes were pre-blocked with a Tris-buffered salt (20 mM Tris, pH 7.5; 150 mM NaCl) containing 5% (w/v) milk powder and 0.01% (w/v) Tween 20. Membranes were probed with the following antibodies raised against: PsbA at 1:2000 dilution; PsbA at 1:5000 dilution; Cyt *f* at 1:2000 dilution; β -ATPase at 1:1000 dilution; Lhcb 1 at 1:2000 dilution; Lhcb2 at 1:2000 dilution. Polyclonal phosphothreonine (Ph-Thr) antibody (Zymed Laboratories Inc.) was used at 1:5000 dilution to immunodetect thylakoid phosphoproteins. After incubation with the secondary antibody conjugated with horseradish peroxidase (Sigma, 1:20 000 dilution), the antibody–protein complexes were visualized by incubation of the blots in ECL chemiluminescent detection reagents (Amersham) and developed on X-Omat film (VWR).

2.3. Low temperature (77 K) fluorescence

Low temperature (77 K) Chl fluorescence emission spectra were collected using a PTI LS-100 fluorometer (Photon Technology International, South Brunswick, NJ, USA) [16]. Corrected Chl fluorescence emission spectra of whole cells of *C. raudensis* were excited at 436 nm 472 nm and recorded using slit width of 4 nm for both excitation and emission. Chl concentration was 10–12 $\mu\text{g/mL}$. All spectra represent an average of two replicates from a single experiment with two scans within each replicate.

2.4. Room temperature chlorophyll fluorescence

In vivo steady-state room temperature, Chl *a* fluorescence induction curves of dark-adapted (15 min) exponentially growing cell cultures was measured using a pulse amplitude modulated Chl fluorescence detection system PAM 101 (Heinz Walz GmbH, Effeltrich, Germany) as described in [19]. Chl fluorescence at open PSII centers (F_o) was excited by a modulated measuring beam (650 nm, 0.12 $\mu\text{mol photons m}^{-2} \text{ s}^{-1}$) at 1.6 kHz in the dark and 100 kHz in the light. Maximum fluorescence at closed PSII centers (F_m) in a dark-adapted state was induced by saturating white light pulses (800 ms, 7500 $\mu\text{mol photons m}^{-2} \text{ s}^{-1}$) provided by a Schott lamp (KL 1500, Schott Glaswerke, Mainz, Germany). Maximum photochemical efficiency (F_v/F_m) was calculated as $(F_m - F_o)/F_m$. After exposure to white actinic light, the saturating pulses were superimposed at 30 s intervals to obtain F_m' (maximum fluorescence in the light-adapted state). All measurements were performed at the corresponding growth temperature using a water-jacketed cuvette. Sodium bicarbonate (10 mM) was added to each sample prior to dark-acclimation. Fluorescence parameters were calculated during steady state photosynthesis using the equations described by Kramer et al. [8] $\Phi_{\text{PSII}} = (F_m' - F_s)/F_m'$

$\Phi_{\text{NO}} = 1/[\text{NPQ} + 1 + qL (F_m/F_o - 1)]$, $\Phi_{\text{NPQ}} = 1 - \Phi_{\text{PSII}} - \Phi_{\text{NO}}$, where Φ_{PSII} is the yield of photochemistry, Φ_{NPQ} is the yield of nonphotochemical dissipation by down-regulation through antenna quenching whereas Φ_{NO} is the yield of all other processes involved in non-photochemical energy losses.

2.5. Pigment analysis and epoxidation states

Algal cells were harvested by centrifugation and pigments were extracted with 100% acetone at 4 °C as in [16]. Pigments were separated and quantified by high-performance liquid chromatography (HPLC) as described previously [31,32]. The system contained a Beckman System Gold programmable solvent module 126, diode array detector module 168 (Beckman Instruments, San Ramon, CA, USA), CSC-Spherisorb ODS-1 reverse phase column (5 μm particle size, 25 \times 0.46 cm I.D.) with an Upchurch Perisorb A guard column (both columns from Chromatographic Specialties Inc., Concord, ON, Canada). Pigments were eluted isocratically for 6 min with a solvent system acetonitrile: methanol: 0.1 M Tris–HCl (pH 8.0), (72:8:3.5, v/v/v), followed by a 2 min linear gradient to 100% methanol:hexane (75:25, v/v) which continued isocratically for 4 min at a flow rate of 2 $\text{cm}^3 \text{ min}^{-1}$. The total pool sizes of the xanthophyll cycle pigments, violaxanthin (V), antheraxanthin (A) and zeaxanthin (Z) were calculated as mmols per 100 mol Chl *a* and the relative epoxidation state (EPS) of the xanthophyll cycle was calculated as $(V + 0.5A)/(V + A + Z)$ [33].

3. Results

3.1. Temperature effects on growth

Table 1 shows the effects of steady state growth temperature on the maximum exponential growth rates of *C. raudensis*. UWO 241 exhibited highest growth rates at 8 °C (Table 1) but failed to grow at 28 °C (data not shown), whereas SAG 49.72 had the highest growth rate at 28 °C (Table 1), and failed to grow at temperatures below 10 °C (data not shown). These data are consistent with previous reports for the psychrophilic strain [16] and we show for the first time that SAG 49.72 is indeed a mesophilic strain of *C. raudensis*. At temperatures between 8° and 11 °C, UWO 241 exhibited exponential growth rates that were 50 to 100% greater than SAG 49.72 at its lowest permissive growth temperature of 11 °C (Table 1). Conversely, at temperatures of 20 °C or higher, SAG 49.72 exhibited exponential growth rates that were 4-fold greater than UWO 241 at its highest permissive growth temperature of 16 °C (Table 1).

Low temperature (77 K) fluorescence emission spectra were collected to confirm the psychrophilic and mesophilic nature of UWO 241 and SAG 49.72 grown at their optimal temperatures (Fig. 1). Regardless of whether Chl *a* (Fig. 1A) or Chl *b* (Fig.

Table 1
The effect of temperature on growth rates of *C. raudensis*

	Growth temperature	Growth rate	Chlorophyll <i>a/b</i> ratio	F_v/F_m
UWO 241	8 °C	0.0986	1.94 \pm 0.05	0.684 \pm 0.003
	11 °C	0.0727	2.23 \pm 0.10	0.659 \pm 0.008
	16 °C	0.0483	2.12 \pm 0.11	0.626 \pm 0.019
SAG 49.72	11 °C	0.0525	3.34 \pm 0.13	0.675 \pm 0.010
	20 °C	0.2009	3.10 \pm 0.09	0.691 \pm 0.013
	28 °C	0.2263	3.01 \pm 0.12	0.741 \pm 0.060

Growth curves were established at 8 °C, 11 °C and 16 °C for the UWO 241 strain, and at 11 °C, 20 °C and 28 °C for the SAG 49.72 strain, as a measure of total chlorophyll (Chl *a* and Chl *b*). All cell cultures were grown at a light intensity of 150 $\mu\text{mol photons m}^{-2} \text{ s}^{-1}$. Growth rates are expressed as $\mu\text{g Chl h}^{-1}$.

1B) was excited, UWO 241 (solid lines) exhibited 77 K fluorescence emission maxima at 682 and 696 nm associated with PSII but minimal fluorescence emission in the region of 713 nm associated with PSI as previously reported [16,19]. However, *C. raudensis* SAG 49.72 (broken lines) exhibited the expected 77 K fluorescence emission maxima at 682 and 696 nm associated with PSII and at 713 nm associated with PSI (Fig. 1) similar to that obtained for the model green alga, *C. reinhardtii* [5,16]. Thus, we show for the first time that the psychrophilic strain, UWO 241, not only exhibits significant differences in energy distribution between PSII and PSI compared to the model green alga, *Chlamydomonas reinhardtii* [5,16], but also compared to the mesophilic strain, SAG 49.72, of *Chlamydomonas raudensis* (Fig. 1).

3.2. Chl *a* fluorescence induction

Fig. 2A and B illustrate examples of Chl *a* fluorescence induction traces obtained for UWO 241 and SAG 49.72, respectively, grown at their optimal growth temperatures but measured at either low ($20 \mu\text{mol photons m}^{-2} \text{s}^{-1}$) and or high ($1000 \mu\text{mol photons m}^{-2} \text{s}^{-1}$) actinic light intensities. During illumination of UWO 241 cells with low actinic light (Fig. 2A), each saturating flash was followed by a transient quenching of F_s , which appeared to recover within 30 s before the next flash. This transient quenching phenomenon of F_s was not observed in SAG 49.72 grown at 28 °C and exposed to low actinic illumination (Fig. 2B; 20). After the onset of actinic illumination (Fig. 2A, up arrow) of UWO 241 at high irradiance at 8 °C (Fig.

2A, 1000), F_s initially decayed rapidly to the F_o level which was associated with an almost complete quenching of F'_m . In addition, F'_o was quenched followed by a rapid recovery in UWO 241 (Fig. 2A, 1000) after the actinic beam was turned off (Fig. 2A, down arrow). In UWO 241, the F_o level increased in response to increased actinic illumination (Fig. 2A). In contrast to UWO 241, SAG 49.72 exhibited an increase in F_s upon exposure to an actinic irradiance of $1000 \mu\text{mol photons m}^{-2} \text{s}^{-1}$ at its optimal growth temperature of 28 °C with no apparent quenching of F'_o (Fig. 2B, 1000).

Since the data in Fig. 2A and B were collected at the respective optimal growth temperatures for UWO 241 (8 °C) and SAG 49.72 (28 °C), we assessed the potential effects of differential growth temperature on the short-term Chl *a* fluorescence induction curves by growing UWO 241 and SAG 49.72 at the common but sub-optimal growth temperature of 16 °C (Fig. 2C and D). Growth at 16 °C caused a minimal 9% decrease in F_v/F_m compared to growth at 8 °C for UWO 241 (Table 1). A similar effect on F_v/F_m was observed for SAG 49.72 grown at 16 °C (data not shown) compared to 28 °C (Table 1). However, growth and the measurement of Chl *a* fluorescence induction at 16 °C exacerbated the transient quenching of F_s in UWO 241 exposed to low light (Fig. 2C, 20), induced significant quenching of F'_o and increased F_o compared to growth at 8 °C and exposure to low actinic irradiance (Fig. 2A, 20). In contrast, minimal effects were observed for SAG 49.72 grown and measured at 16 °C but low actinic irradiance (Fig. 2D, 20) compared to growth and measurement of Chl *a* fluorescence at 28 °C (Fig. 2B, 20). Exposure of UWO 241 to high actinic irradiance at 16 °C induced an even greater quenching of F_s and F'_o (Fig. 2C, 1000) than observed at 8 °C (Fig. 2A, 1000). Minimal differences were observed between SAG 49.72 measured at 16 °C and high actinic irradiance (Fig. 2D, 1000) compared to 28 °C (Fig. 2C, 1000). These data indicate significant differences in the sensitivity of the photosynthetic fluorescence induction curves to both temperature and measuring irradiance in the psychrophilic and mesophilic strains of the same species. Furthermore, the qualitative differences in these fluorescence induction curves between UWO 241 and SAG 49.72 cannot be accounted for by simple differences in growth temperatures.

3.3. Growth temperature and energy partitioning

To quantify the potential differences in energy partitioning between the mesophile and the psychrophile, we examined the long-term effects of growth temperature on photochemical and non-photochemical quenching processes (Fig. 3). UWO 241 grown at its optimal temperature of 8 °C exhibited comparable excitation pressure, measured as 1-qL, as that observed for SAG 49.72 grown at its optimal temperature of (28 °C) (Fig. 3A). In both strains, 1-qL increased as growth temperature decreased. However, 1-qL for UWO 241 at its sub-optimal growth temperature of 16 °C was almost 50% lower than that of SAG 49.72 at its sub-optimal growth temperature of 11 °C (Fig. 3A).

At its optimal growth temperature of 8 °C, the photochemical yield of PSII (Φ_{PSII}) in UWO 241 was about 30% lower than that of SAG 49.72 at 28 °C (Fig. 3B, grey shaded areas). This

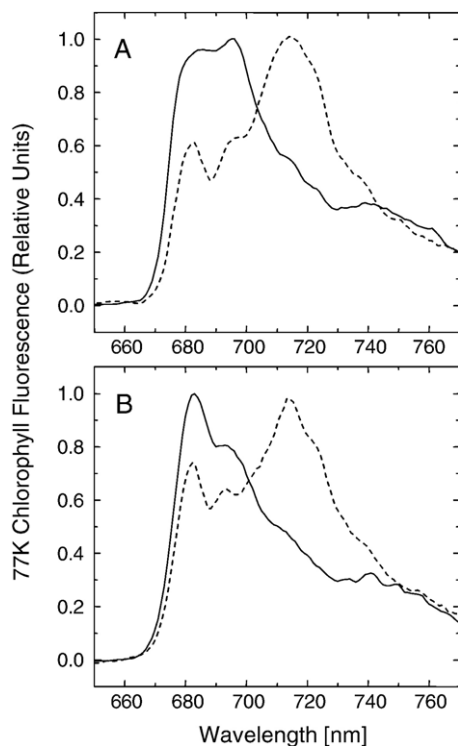


Fig. 1. 77 K fluorescence emission spectra of the psychrophilic (solid line) and mesophilic (dotted line) strains of *C. raudensis* grown at the optimal temperatures of 8 °C and 28 °C, respectively. Emission spectra were obtained for (A) Chl *a* and (B) Chl *b* excitation at 436 and 472 nm, respectively.

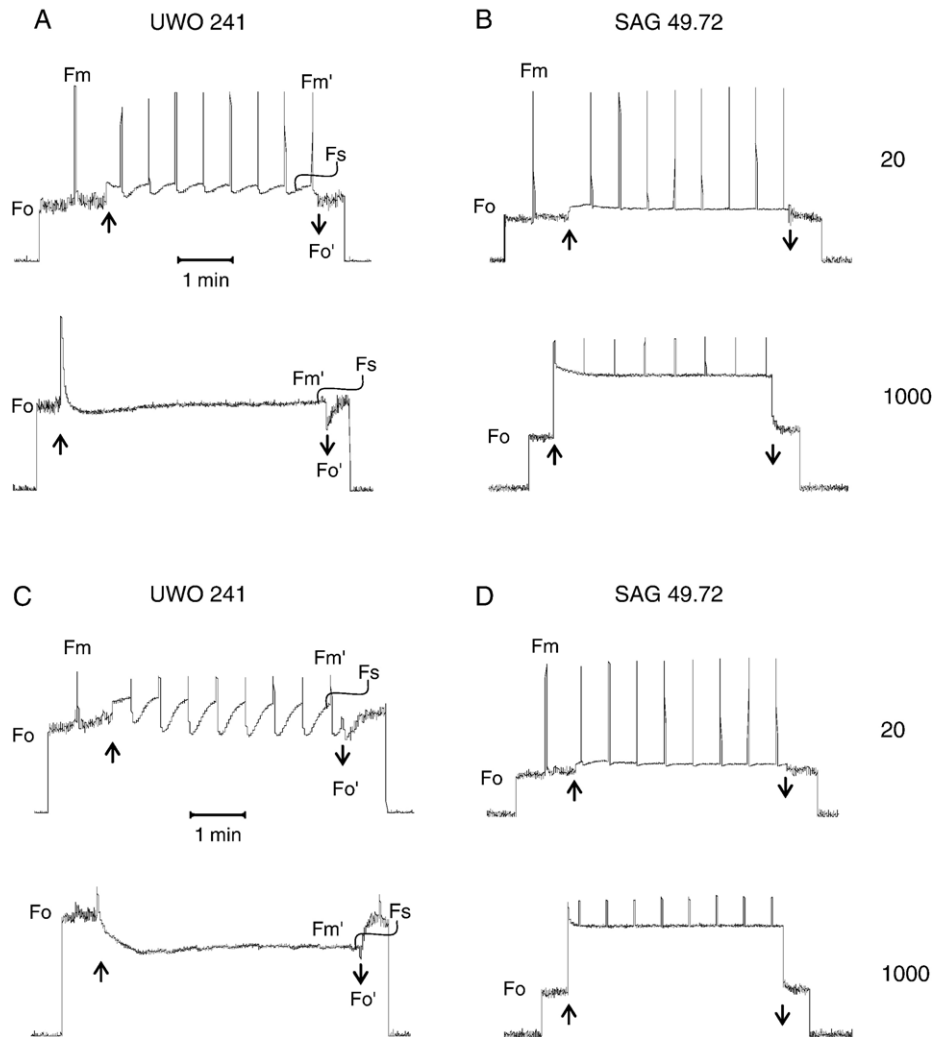


Fig. 2. Typical chlorophyll fluorescence induction traces of *C. raudensis* cells illustrating the effects of short-term measuring light intensities (as indicated in $\mu\text{mol m}^{-2} \text{s}^{-1}$). UWO 241 and SAG 49.72 strains were grown and measured at their optimal growth temperatures of 8 °C and 28 °C, respectively (A and B) and at a common suboptimal temperature of 16 °C (C and D). Cells were dark adapted for 15 min prior to collection of the fluorescence traces. (↑) Actinic light on. (↓) Actinic light off.

appeared to be due to the fact that UWO 241, at its optimal growth temperature, exhibited almost a 2-fold greater Φ_{NPQ} (Fig. 3B, white shaded areas) than that of SAG 49.72 at 28 °C with comparable levels of Φ_{NO} (Fig. 3B, black shaded areas). As growth temperature increased for UWO 241 from 8° to its sub-optimal temperature of 16 °C, Φ_{PSII} decreased with a concomitant increase in total non-photochemical quenching capacity ($\Phi_{\text{NPQ}} + \Phi_{\text{NO}}$) due, by and large, to a doubling in Φ_{NO} (Fig. 3B). Although similar trends were observed for the decrease in Φ_{PSII} of SAG 49.72 grown at 28 °C compared to growth at its sub-optimal temperature of 11 °C (Fig. 3B), this was due, by and large to a doubling of Φ_{NPQ} with minimal changes in Φ_{NO} (Fig. 3B).

3.4. Growth irradiance and energy partitioning

In response to increasing steady state growth irradiance from 20 to 500 $\mu\text{mol photons m}^{-2} \text{s}^{-1}$ at their respective optimal growth temperatures, both UWO 241 and SAG 49.72 exhibited a 3-fold increase in 1-qL (Fig. 4A). This was accompanied by an

87% decrease in Φ_{PSII} (Fig. 4B) and a concomitant doubling in both Φ_{NPQ} (Fig. 4C) and Φ_{NO} (Fig. 4D) for UWO 241. In contrast, SAG 49.72 exhibited a decrease in Φ_{PSII} of only 28% over the same range of growth irradiance (Fig. 4B), a doubling in Φ_{NPQ} (Fig. 4C) but only a 25% increase in Φ_{NO} (Fig. 4D).

3.5. Xanthophyll cycle activity

Since the xanthophyll cycle plays an important role in the regulation of NPQ [33], the epoxidation states of the xanthophyll cycle pigments were quantified for UWO 241 and SAG 49.72 grown at various growth temperatures (Fig. 5A) and growth irradiance (Fig. 5B). Epoxidation states of the two strains were highest at close to optimal growth temperatures and lowest at suboptimal temperatures for UWO 241 and for SAG 49.72 (Fig. 5A).

The data in Fig. 5B illustrate that both the psychrophile and the mesophile have an active xanthophyll cycle that is sensitive to growth irradiance. As growth irradiance increased, the epoxidation state in both strains decreased as expected.

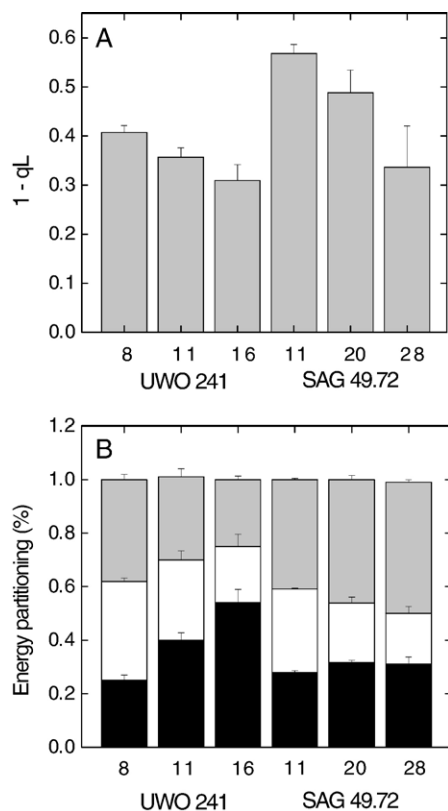


Fig. 3. PSII excitation pressure, as estimated by 1-qL (A) for UWO 241 grown at 8, 11 and 16 °C and SAG 49.72 grown at 11, 16, 20 and 28 °C. (B) Energy partitioning at PSII during different growth temperatures of both strains of *C. raudensis*. Bars indicate the relative yields of Φ_{NO} =non-regulated dissipation (black), Φ_{NPQ} =non-photochemical quenching (white) and Φ_{PSII} =efficiency of PSII (grey). Cultures were grown at an irradiance of 150 $\mu\text{mol photons m}^{-2} \text{s}^{-1}$. Parameters were determined according to Kramer et al. [8].

However, for a given irradiance, the epoxidation state was always lower in UWO 241 than SAG 49.72 which is consistent with the greater NPQ observed for the psychrophile (Fig. 4A) than the mesophile (Fig. 4B) at their respective optimal growth temperatures.

3.6. Photosystem stoichiometry

During growth at various temperature and light regimes, the abundance of specific thylakoid polypeptides was analysed (Fig. 6 and 7), including PsaA (the photosystem I heterodimer), PsbA (the reaction center protein of photosystem II), cytochrome *f* (Cyt *f*) of the cytochrome b_6f complex, the β -subunit of ATPase (β -ATPase), and two major light harvesting polypeptides of LHCII, Lhcb1 and Lhcb2. Consistent with the 77 K fluorescence data, immunoblot analysis confirmed the presence of low levels of PSI in the psychrophilic strain, UWO 241, relative to SAG 49.72 at the optimal temperatures of 8 °C and 28 °C, respectively (Fig. 6). In response to growth under increasing temperatures, UWO 241 exhibited an increase in PsaA abundance relative to PsbA, indicative of an increase in the PSI/PSII ratio. However, minimal changes were observed with respect to the contents of Cyt *f*, β -ATPase, Lhcb1 and

Lhcb2 in response to increasing growth temperature in UWO 241 (Fig. 6). In contrast, SAG 49.72 exhibited no significant changes in the amount of either PsaA or PsbA as a function of decreasing growth temperature (Fig. 6). Furthermore, the abundance of Cyt *f*, β -ATPase, Lhcb1 and Lhcb2 appeared to increase relative to either PsaA or PsbA in SAG 49.72 as a function of decreasing growth temperature (Fig. 6). Although growth temperature had minimal effects on the Chl *a/b* ratios of both UWO 241 and SAG 49.72, the Chl *a/b* ratio of SAG 49.72 was almost double that of UWO 241 (Table 1) which is similar to the differences observed between UWO 241 and the model mesophile, *C. reinhardtii* [5,16].

In contrast to growth temperature, both strains of *C. raudensis* exhibited minimal changes in PsaA and PsbA in response to increasing growth irradiance at optimal growth temperatures (Fig. 7). Both *C. raudensis* strains showed increasing levels of Cyt *f* and β -ATPase with increasing growth irradiance (Fig. 7). Consistent with previous results for photoacclimation in mesophilic species [5,14,25,34,35], both UWO 241 as well as SAG 49.72 exhibited a reduction in the level of both Lhcb1 and Lhcb2 with increasing growth irradiance. However, SAG 49.72 appeared to be more sensitive to a high light-induced reduction in Lhcb1 and Lhcb2 content than UWO 241 (Fig. 7). This was accompanied by a 15% increase in Chl *a/b* ratios from 1.83 ± 0.06 at 30 $\mu\text{mol photons m}^{-2} \text{s}^{-1}$ to 2.10 ± 0.06 at 500 $\mu\text{mol photons m}^{-2} \text{s}^{-1}$ for UWO 241 while for SAG 49.72, the Chl *a/b* increased from 2.75 ± 0.06 to 3.23 ± 0.11 over the same irradiance.

3.7. Polypeptide phosphorylation profiles

Phosphorylation profiles of thylakoid polypeptides under varying growth temperatures and a constant growth irradiance of 150 $\mu\text{mol photons m}^{-2} \text{s}^{-1}$ exhibited major differences between the two strains of *C. raudensis* (Fig. 8). *C. raudensis* UWO 241 exhibited prominent threonine phosphorylation of a high molecular mass polypeptide in the range of 115 kDa but no apparent threonine phosphorylation of polypeptides in the molecular mass range of 30 kDa associated with LHCII polypeptides (Fig. 8A). The extent of phosphorylation of this polypeptide appeared to be insensitive to growth temperature (Fig. 8A) and migrated coincidentally with the Chl *a*-protein complex typically associated with PSI in SDS-PAGE of non-heated thylakoid samples (data not shown). However, the LHCII polypeptides with an apparent molecular mass in the range of 30 kDa were the major polypeptides phosphorylated at all growth temperatures in SAG 49.72 (Fig. 8A). In addition, threonine phosphorylation of a 47 kDa polypeptide as well as a polypeptide of about 115 kDa were observed in SAG 49.72. However, the extent of threonine phosphorylation in SAG 49.72 appeared to be temperature dependent with the highest level of phosphorylation observed at the sub-optimal growth temperature of 11 °C (Fig. 8A).

As a function of increasing irradiance at optimal growth temperatures, threonine phosphorylation of LHCII associated polypeptides of approximately 30 kDa was again observed only in the SAG 49.72 strain and the level of phosphorylation of the

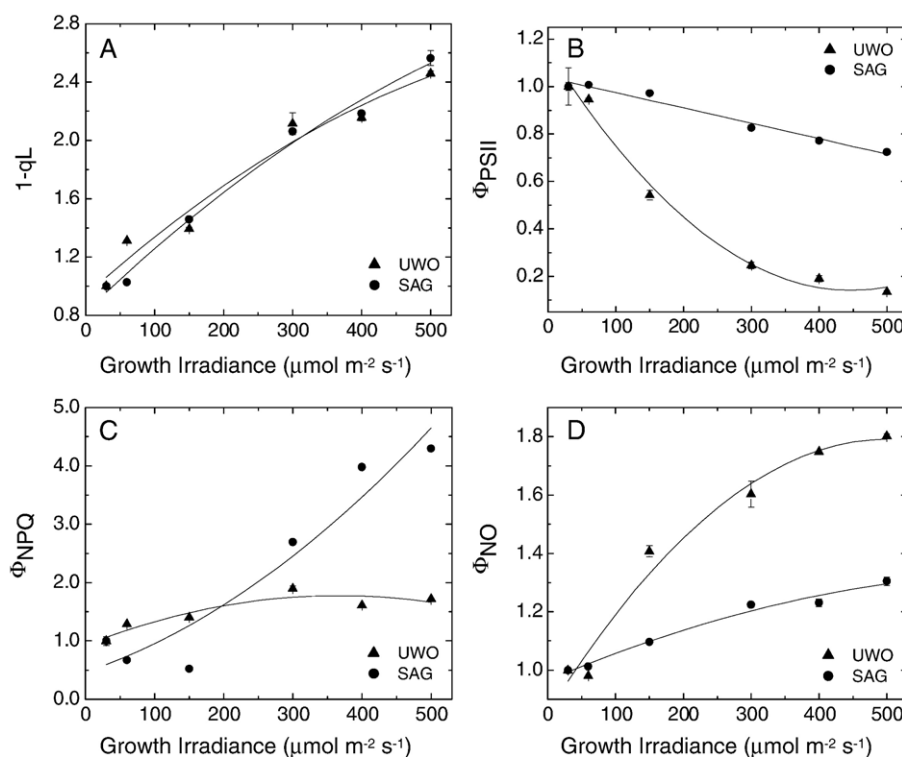


Fig. 4. Energy partitioning at PSII under various growth irradiance regimes for UWO 241 (●) and SAG 49.72 (▲). Normalized values are presented for changes in Φ_{II} =efficiency of PSII (A), $1-qL$ =excitation pressure (B), Φ_{NPQ} =non-photochemical quenching (C), and Φ_{NO} =non-regulated dissipation (D) in response to changing growth light. Cultures were grown at the optimal temperatures of 8 °C and 28 °C for UWO 241 and SAG 49.72, respectively. Parameters were determined according to Kramer et al. [8].

30 kDa polypeptides decreased with increasing growth irradiance (Fig. 8B). The phosphorylation of high molecular mass polypeptides in UWO 241 was undetectable at a growth irradiance of 30 $\mu\text{mol photons m}^{-2} \text{s}^{-1}$ but increased with increased growth irradiance with maximum threonine phosphorylation occurring between 300 and 400 $\mu\text{mol photons m}^{-2} \text{s}^{-1}$ (Fig. 8B).

4. Discussion

The growth kinetic data presented in Table 1 indicate that SAG 49.72 is the mesophilic strain of *Chlamydomonas raudensis* since it exhibited optimal growth temperatures around 28 °C and was unable to grow below 11 °C. The growth data presented for UWO 241 are consistent with previous reports indicating that it is the psychrophilic strain of *C. raudensis* [5,16]. A comparison of excitation pressure ($1-qL$) at their respective optimal growth temperatures indicates photosynthetic adaptation of UWO 241 and SAG 49.72 to low and high growth temperature respectively. As expected, $1-qL$ increased with a decrease in growth temperature in both strains of *C. raudensis* (Fig. 3A). However, excitation pressure exhibited by UWO 241 at its optimal growth temperature of 8 °C is comparable to that of SAG 49.72 at its optimal growth temperature of 28 °C (Fig. 3B). Thus, UWO 241 grown at 8 °C exhibits a comparable energy balance as that of the mesophile grown at 28 °C indicating that both the psychrophile and the

mesophile maintain photostasis at their optimal growth temperature.

However, the mechanism by which the psychrophile and the mesophile maintain photostasis under varying growth temperatures appears to be quite different. As growth temperature is increased to suboptimal maximum values in UWO 241 or decreased to suboptimal minimum values in SAG 49.72, the yield of PSII electron transport decreased (Fig. 3B). This was associated with a decrease in Φ_{NPQ} but a concomitant increase in Φ_{NO} in the psychrophile whereas Φ_{NPQ} increased with minimal changes in Φ_{NO} in the mesophile. Thus, competition for the flux of excitation energy between inducible, down regulatory processes (Φ_{NPQ}) versus other constitutive processes involved in energy dissipation (Φ_{NO}) favours constitutive processes in UWO 241 whereas it favours the down regulatory processes in the mesophile (Fig. 3B).

Not only is UWO 241 adapted to low growth temperature but it is also shade adapted [5]. This is consistent with our data which indicate that the Φ_{PSII} in the psychrophile is more sensitive to growth irradiance than the mesophile (Fig. 4B). Furthermore, UWO 241 favours energy partitioning through constitutive energy dissipation processes (Φ_{NO}) rather than inducible NPQ in response to increased growth irradiance. We suggest that these differences in the regulation of energy partitioning processes between UWO 241 and SAG 49.72 account for the significant differences observed in the fluorescence quenching in the Chl *a* induction curves (Fig. 2).

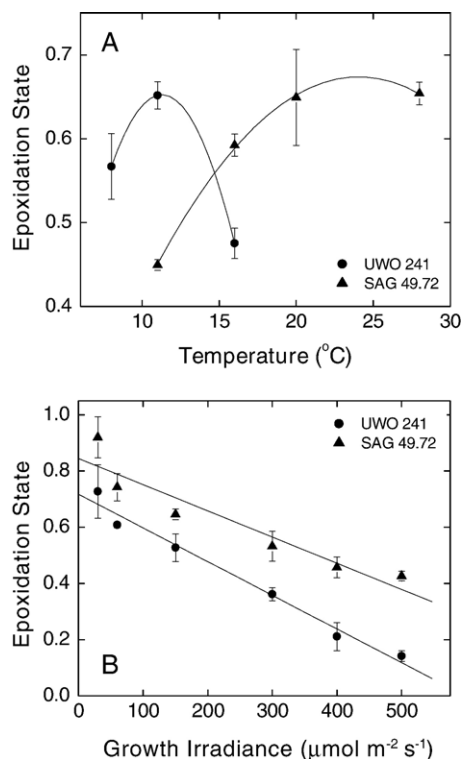


Fig. 5. Epoxidation states ($EPS = (V + 0.5A/V + Z)$) of *Chlamydomonas raudensis* UWO 241 (●) and SAG 49.72 (▲) during steady-state growth at various temperatures (A) and light intensities (B). Cells were grown at $150 \mu\text{mol photons m}^{-2} \text{s}^{-1}$ for all growth temperature treatments (A) and at the optimal temperatures of 8 °C and 28 °C (B) for UWO 241 and SAG 49.72 for all growth irradiance regimes.

We conclude that photostasis is maintained primarily through constitutive dissipative processes rather than inducible energy dissipative processes in the psychrophile in response to either suboptimal growth temperature or increased growth irradiance.

Antenna quenching through the xanthophyll cycle is considered to be the primary, inducible, down-regulatory process controlling nonphotochemical energy dissipation in autotrophic eukaryotes [33]. We show for the first time that the temperature profile of the xanthophyll cycle is the inverse of the growth response of an organism (Fig. 5A). EPS is highest at the optimal growth temperature for both the mesophile and the psychrophile which indicates that xanthophyll cycle activity is minimal under optimal growth conditions but maximal at non-permissive growth temperature. This is consistent with the fact that photosynthetic rates are maximal at the optimal growth temperatures for the psychrophile and mesophile [36]. This indicates that the xanthophyll cycle is adapted to optimal growth temperatures rather than to the absolute growth temperature.

The response of the xanthophyll cycle to growth irradiance was similar for UWO 241 and SAG 49.72 (Fig. 5B). Thus, antenna quenching through the xanthophyll cycle cannot account for the differential quenching between the psychrophile and the mesophile in response to irradiance (Fig. 2). This is supported by the fact that F_o fluorescence in UWO 241 increased rather than decreased in response to actinic irradiance

(Fig. 2). The latter would indicate antenna quenching [10]. Since F_o increases in UWO 241, this would indicate that PSII in UWO 241 is more sensitive to photodamage than SAG 49.72 [10]. Since UWO 241 is locked in state 1 [17], the differential quenching exhibited by the psychrophile cannot be accounted for by a higher capacity for state transitions in UWO 241 than SAG 49.72. We suggest that the differential quenching observed in the psychrophile may reflect either differential zeaxanthin-independent antenna quenching [37] or differential PSII reaction centre quenching [10]. The present data do not allow us to distinguish between these two possible alternatives.

An examination of the chlorophyll fluorescence induction curves (Fig. 2) also revealed an increase in the fluorescence intensity after the actinic light was turned off in UWO 241 but not in SAG 49.72. Such a response may be interpreted to indicate a differential reduction of the PQ pool due to either cyclic PSI electron transport or chlororespiration [38,39]. Therefore, suboptimal growth temperatures and increased irradiance may result in higher levels of chlororespiration and/or cyclic electron flow around PSI in UWO 241. These trends correlate with increased levels of non-regulated dissipation, as well as decreased epoxidation states in UWO 241. This may occur because both chlororespiration [38] and cyclic electron flow significantly contribute to the generation of a pH gradient across the thylakoid membrane [39].

The regulation of photosystem stoichiometry is an important mechanism in the regulation of photostasis [14,15]. Morgan-Kiss et al. [19] demonstrated that UWO 241 is able to adjust photosystem stoichiometry in response to light quality. In

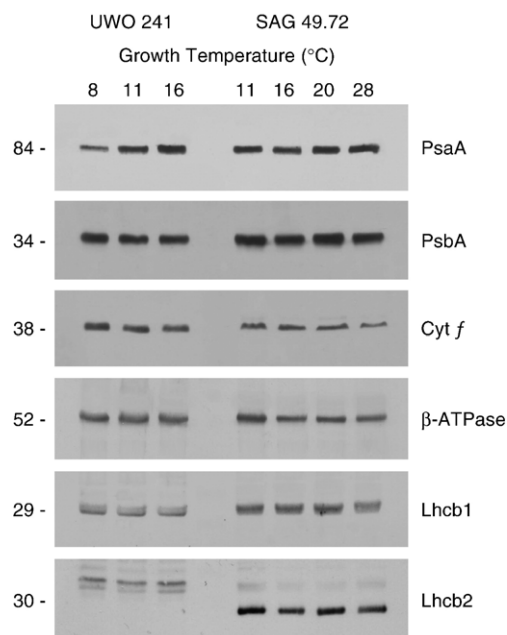


Fig. 6. Immunoblot analysis of specific thylakoid membrane polypeptides of *C. raudensis* UWO 241 and SAG 49.72 in response to steady-state growth temperatures. SDS-PAGE separated thylakoid proteins were probed with antibodies raised against PsbA, PsbA (D1), Cyt *f*, β-ATPase, Lhcb1 and Lhcb2 polypeptides. Numbers above lanes represent growth temperature (°C). All cells were grown under an irradiance of $150 \mu\text{mol photons m}^{-2} \text{s}^{-1}$. Lanes of SDS-PAGE were loaded on an equal Chl basis.

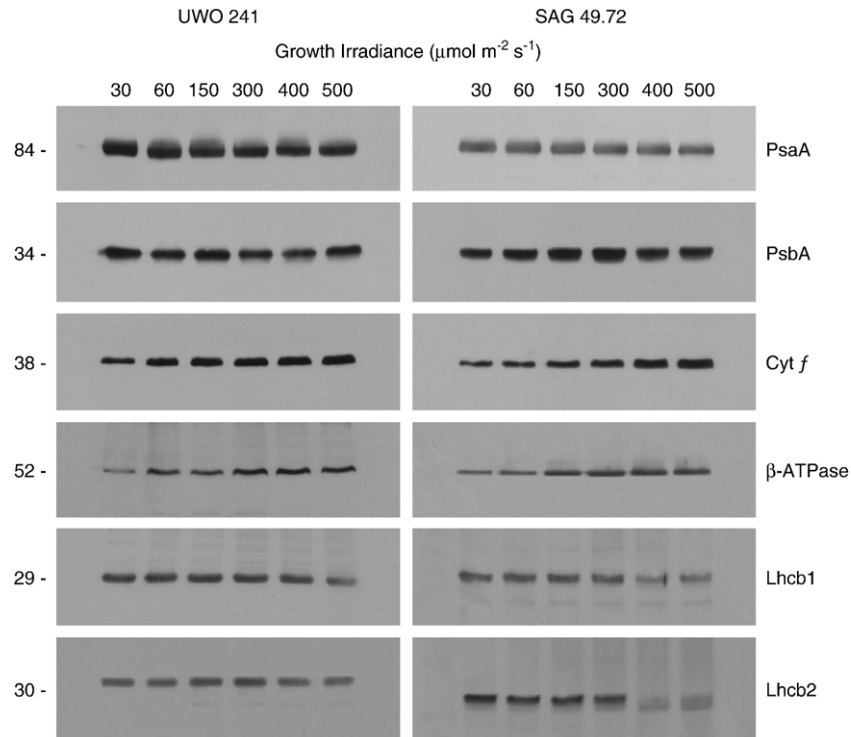


Fig. 7. Immunoblot analysis of specific thylakoid membrane polypeptides isolated from *C. raudensis* UWO 241 (left column) and SAG 49.72 (right column) in response to growth light intensity. Cells were grown at the optimal temperatures of 8 °C and 28 °C for UWO 241 and SAG 49.72, respectively. Numbers above lanes represent growth irradiance in $\mu\text{mol photons m}^{-2} \text{s}^{-1}$.

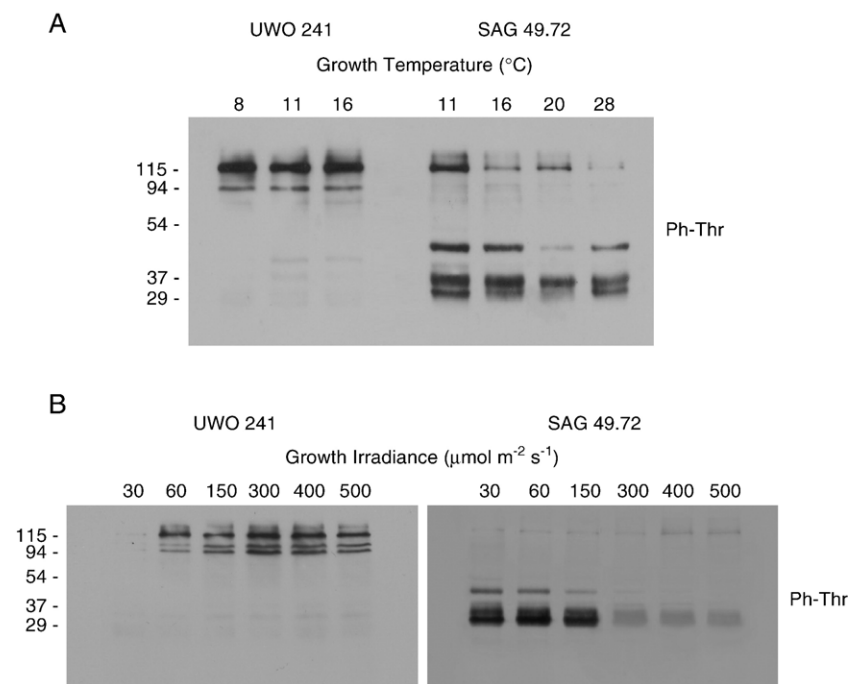


Fig. 8. Phosphorylation profiles of thylakoid membrane polypeptides of *C. raudensis* in response to growth temperature (A) and growth irradiance (B), as represented by the values (in °C and $\mu\text{mol photons m}^{-2} \text{s}^{-1}$) above each lane. Immunodetection was performed by using antibodies raised against phospho-threonine (Ph-Thr). During growth temperature experiments, cells were exposed to a light intensity of 150 $\mu\text{mol photons m}^{-2} \text{s}^{-1}$, and growth irradiance experiments were performed at the optimal temperatures of 8 °C for UWO 241 and 28 °C for SAG 49.72.

addition to light quality, we show that *C. raudensis* UWO 241 is able to regulate PSI/PSII stoichiometry under long-term steady state growth under various temperature regimes. As growth conditions approach a non-permissive temperature, the abundance of PSI increases in the psychrophilic strain relative to PSII. Adjustments in photosystem stoichiometry are considered to be regulated specifically by the redox state of the plastoquinone pool [40,41]. When PSI limits the rate of electron transport, the PQ pool is largely in a reduced state which activates the expression of *psaA/B*, and when PSII is rate-limiting, the PQ pool is largely oxidized which activates the expression of *psbA* and inhibits that of *psaA/B* [28]. However, the data obtained for both strains of *C. raudensis* are not consistent with this model. Growth under increased light intensity in both strains and low growth temperatures for UWO 241 correlates with lower levels of PSI and higher excitation pressure as measured by 1-qL. Although growth under higher irradiance at optimal temperatures results in minimal decreases of PSI abundance, growth at a common, suboptimal temperature for both strains results in a greater reduction of PSI (data not shown). In addition, low levels of PSI are correlated not only with higher excitation pressure, but also an increase in the abundance of the Cyt *b₆f* complex. The trends in the abundance of PSI and Cyt *b₆f* observed in UWO 241 polypeptides are identical to the results obtained for steady state growth under various light and temperature regimes for the cyanobacterium *Plectonema boryanum* UTEX 485 [40]. In contrast to regulation of PSI/PSII by the PQ pool, studies with the cyanobacterium *Synechocystis* PCC 6714 suggest that photosystem stoichiometry is controlled by the redox state of the Cyt *b₆f* complex, which regulates translation of the *psaAB* genes [41]. It has also been suggested that in *P. boryanum*, the redox sensor for acclimation seems to be localized downstream of the Cyt *b₆f* complex [40]. However, it should be noted that cyanobacteria are the only organisms that perform photosynthetic and respiratory electron transport within the same cell compartment where they share some common components, including the PQ pool and the Cyt *b₆f* complex [42,43]. Therefore, reduction of the PQ pool may occur by stromal electron sources via NADH dehydrogenases and cyclic electron flow around PSI in addition to reduction by PSII [40]. In the case of UWO 241 and *Synechocystis*, low levels of PSI occur during growth at high irradiance and low temperatures, two conditions that tend to cause an imbalance in photostasis, characterized by an overreduction of the PQ pool [6]. As a result, electron transport may be limited due to a limitation on the acceptor side of PSI.

Phosphorylation of LHCII polypeptides is essential in the regulation of state transitions and energy distribution between PSII and PSI [18]. In contrast to SAG 49.72, UWO 241 does not exhibit the capacity to phosphorylate LHCII polypeptides in response to either growth temperature or growth irradiance (Fig. 8A). This is consistent with the reports that UWO 241 exhibits minimal LHCII phosphorylation even in response to conditions which induce state transitions in green algae [19]. Rather, UWO 241 exhibits phosphorylation of high molecular mass polypeptides, comparable to that of the PSI complex and/or the associated proteins which have been reported previously [19].

The data presented here confirm that this distinct phosphorylation profile is specific to UWO 241 and not to *C. raudensis* as a species. PSI-D was recently reported to be the first phosphorylated PSI subunit detected along with another protein with an unknown function, designated as PSI-P [44].

In response to increasing growth irradiance, phosphorylation of LHCII associated polypeptides in the SAG 49.72 strain decreased. This suggests high-light-induced inactivation of the LHCII-associated kinase. Previous studies have shown that maximal phosphorylation of LHCII polypeptides *in vivo* occurs at low light intensities and thus, a strong down-regulation of phosphorylation takes place at higher irradiances [45]. Consistent with these findings, recent reports have suggested that the mechanism of state transitions may only be physiologically important at low light intensities [46]. In contrast, the phosphorylation of high molecular mass polypeptides in UWO 241 increased with increased growth irradiance with a maximum between 300 and 500 $\mu\text{mol photons m}^{-2} \text{s}^{-1}$ (Fig. 8B). We suggest that the phosphorylation of these high molecular mass polypeptides in UWO 241 must occur by a protein kinase distinct from the LHCII kinase.

In summary, adaptation of UWO 241 to low temperature and low growth irradiance has resulted in alterations in the partitioning of excess excitation energy to maintain photostasis. While the mesophile, SAG 49.72, favours energy partitioning through typical inducible, down regulatory processes (Φ_{NPQ}) associated with the xanthophyll cycle and antenna quenching, the psychrophilic strain of the same species, UWO 241, favours energy partitioning through other constitutive processes involved in energy dissipation (Φ_{NO}) in response to both growth temperature and growth irradiance. The molecular basis of these constitutive quenching processes for photoprotection and photostasis has yet to be elucidated. However, these constitutive quenching processes may be related to phosphorylation of high molecular mass polypeptides putatively associated with PSI. Since we have compared a psychrophile and a mesophile of the same rather than of different species, this strengthens our thesis that the distinct differences in photoacclimation between *Chlamydomonas raudensis* UWO 241 and SAG 49.72 reflect differences due to psychrophily rather than to species differences. Thus psychrophily in this photoautotroph is complex and involves regulation of energy balance at low temperature in addition to the capacity to synthesize cold-adapted enzymes typically associated with heterotrophs [47,48].

Acknowledgement

This work was financially supported by the National Science and Engineering Research Council of Canada.

References

- [1] P.J. Neale, J.C. Priscu, The photosynthetic apparatus of phytoplankton from a perennially ice-covered Antarctic lake-acclimation to an extreme shade environment, *Plant Cell Physiol.* 36 (1995) 253–263.
- [2] M.P. Lizotte, J.C. Priscu, Spectral irradiance and bio-optical properties in

- perennially ice covered lakes of the dry valleys (McMurdo Sound, Antarctica), *Antarct. Res. Ser.* 57 (1992) 1–14.
- [3] T. Pocock, M.A. Lachance, T. Pröschold, J.C. Priscu, S. Kim, N.P.A. Hüner, Identification of a psychrophilic green alga from Lake Bonney Antarctica: *Chlamydomonas raudensis* Etlt. (UWO 241) (Chlorophyceae), *J. Phycol.* 40 (2004) 1138–1148.
 - [4] G. Öquist, N.P.A. Hüner, Photosynthesis of overwintering evergreen plants, *Annu. Rev. Plant Biol.* 54 (2003) 329–355.
 - [5] R.M. Morgan-Kiss, J.C. Priscu, T. Pocock, L. Gudynaite-Savitch, N.P.A. Hüner, Adaptation and acclimation of photosynthetic microorganisms to permanently cold environments, *Microbiol. Mol. Biol. Rev.* 70 (2006) 222–252.
 - [6] N.P.A. Hüner, G. Öquist, F. Sarhan, Energy balance and acclimation to light and cold, *Trends Plant Sci.* 3 (1998) 224–230.
 - [7] N.P.A. Hüner, G. Öquist, A. Melis, Photostasis in plants, green algae and cyanobacteria: the role of light harvesting antenna complexes, in: B.R. Green, W. Parsons (Eds.), *Light Harvesting Antennae*, Advances in Photosynthesis, vol. 13, Kluwer Academic Publishers, Dordrecht, 2003, pp. 401–422.
 - [8] D.M. Kramer, G. Johnson, O. Kiirats, G.E. Edwards, New fluorescence parameters for the determination of Q_A redox state and excitation energy fluxes, *Photosynth. Res.* 79 (2004) 209–218.
 - [9] G.R. Gray, L.V. Savitch, A.G. Ivanov, N.P.A. Hüner, Photosystem II excitation pressure and development of resistance to photoinhibition: II. Adjustment of photosynthetic capacity in winter wheat and winter rye, *Plant Physiol.* 110 (1996) 61–71.
 - [10] G.H. Krause, E. Weis, Chlorophyll fluorescence and photosynthesis: the basics, *Annu. Rev. Plant Physiol. Plant Mol. Biol.* 42 (1991) 313–349.
 - [11] N.G. Bukhov, U. Heber, C. Wiese, V.A. Shuvalov, Energy dissipation in photosynthesis: does the quenching of chlorophyll fluorescence originate from antenna complexes of photosystem II or from the reaction center? *Planta* 212 (2001) 749–758.
 - [12] S. Matsubara, W.S. Chow, Populations of photoinactivated photosystem II reaction centers characterized by chlorophyll a fluorescence lifetime in vivo, *Proc. Natl. Acad. Sci. U. S. A.* 101 (2004) 18234–18239.
 - [13] A.G. Ivanov, P.V. Sane, M. Krol, G.R. Gray, A. Balseris, L.V. Savitch, G. Öquist, N.P.A. Hüner, Acclimation to temperature and irradiance modulates PSII charge recombination, *FEBS Lett.* 580 (2006) 2797–2802.
 - [14] A. Melis, Dynamics of photosynthetic membrane composition and function, *Biochim. Biophys. Acta* 1058 (1991) 87–106.
 - [15] J. Yamazaki, T. Suzuki, E. Maruta, Y. Kamimura, The stoichiometry and antenna size of the two photosystems in marine green algae, *Bryopsis maxima* and *Ulva pertusa*, in relation to the light environment of their natural habitat, *J. Exp. Bot.* 56 (2005) 1517–1523.
 - [16] R.M. Morgan, A.G. Ivanov, J.C. Priscu, D.P. Maxwell, N.P.A. Hüner, Structure and composition of the photochemical apparatus of the Antarctic green alga, *Chlamydomonas subcaudata*, *Photosynth. Res.* 56 (1998) 303–314.
 - [17] R.M. Morgan-Kiss, A.G. Ivanov, N.P.A. Hüner, The Antarctic psychrophile, *Chlamydomonas subcaudata*, is deficient in state I state II transitions, *Planta* 214 (2002) 435–445.
 - [18] G. Finazzi, G. Forti, Metabolic flexibility of the green alga *Chlamydomonas reinhardtii* as revealed by the link between state transitions and cyclic electron flow, *Photosynth. Res.* 82 (2004) 327–338.
 - [19] R.M. Morgan-Kiss, A.G. Ivanov, T. Pocock, M. Król, L. Gudynaite-Savitch, N.P.A. Hüner, The Antarctic psychrophile, *Chlamydomonas raudensis* Etlt (UWO 241) (Chlorophyceae, Chlorophyta), exhibits a limited capacity to photoacclimate to red light, *J. Phycol.* 41 (2005) 791–800.
 - [20] J.F. Allen, Cytochrome b6f: structure for signalling and vectorial metabolism, *Trends Plant Sci.* 9 (2004) 130–137.
 - [21] A.V. Vener, P.J. van Kan, A. Gal, B. Andersson, I. Ohad, Activation deactivation cycle of redox-controlled thylakoid protein-phosphorylation-role of plastoquinol bound to the reduced cytochrome b6f complex, *J. Biol. Chem.* 270 (1995) 25225–25232.
 - [22] F. Zito, G. Finazzi, R. Delosme, W. Nitschke, D. Picot, F.A. Wollman, The Qo site of cytochrome b6f complexes controls the activation of the LHCI kinase, *EMBO J.* 18 (1999) 2961–2969.
 - [23] T. Pfannschmidt, Acclimation to varying light qualities: toward the functional relationship of state transitions and adjustment of photosystem stoichiometry, *J. Phycol.* 41 (2005) 723–725.
 - [24] J.F. Allen, T. Pfannschmidt, Balancing the two photosystems: photosynthetic electron transfer governs transcription of reaction centre genes in chloroplasts, *Philos. Trans. R. Soc. Lond.* 355 (2000) 1351–1359.
 - [25] P.G. Falkowski, T.G. Owens, A.C. Ley, D.C. Mauzerall, Effects of growth irradiance levels on the ratio of reaction centers in 2 species of marine-phytoplankton, *Plant Physiol.* 68 (1981) 969–973.
 - [26] J. Yamazaki, Y. Kamimura, M. Okada, Y. Sugimura, Changes in photosynthetic characteristics and photosystem stoichiometries in the lower leaves in rice seedlings, *Plant Sci.* 148 (1999) 155–163.
 - [27] A. Melis, A. Murakami, J.A. Nemson, K. Aizawa, K. Ohki, Y. Fujita, Chromatic regulation in *Chlamydomonas reinhardtii* alters photosystem stoichiometry and improves the quantum efficiency of photosynthesis, *Photosynth. Res.* 47 (1996) 253–256.
 - [28] T. Pfannschmidt, J.F. Allen, R. Oelmler, Principles of redox control in photosynthesis gene expression, *Physiol. Plant.* 112 (2001) 1–9.
 - [29] S.W. Jeffrey, G.F. Humphrey, New spectrophotometric equations for determining chlorophyll a, b, cl, c2 in higher plants, algae and natural phytoplankton, *Biochem. Physiol. Pflanzen* 167 (1975) 191–194.
 - [30] U.K. Laemmli, Cleavage of structural proteins during the head of bacteriophage T4, *Nature* 227 (1970) 680–685.
 - [31] A.G. Ivanov, R.M. Morgan, G.R. Gray, M.Y. Velitchkova, N.P.A. Hüner, Temperature/light dependent development of selective resistance to photoinhibition of photosystem I, *FEBS Lett.* 430 (1998) 288–292.
 - [32] A.G. Ivanov, M. Król, D. Maxwell, N.P.A. Hüner, Abscissic acid induced protection against photoinhibition of PS II correlates with enhanced activity of the xanthophyll cycle, *FEBS Lett.* 371 (1995) 61–64.
 - [33] B. Demmig-Adams, W.W. Adams, Photoprotection and other responses of plants to high light stress, *Annu. Rev. Plant Physiol. Plant Mol. Biol.* 43 (1992) 599–626.
 - [34] D.P. Maxwell, S. Falk, N.P.A. Hüner, Photosystem II excitation pressure and development of resistance to photoinhibition: 1. Light-harvesting complex-II abundance and zeaxanthin content in *Chlorella vulgaris*, *Plant Phys.* 107 (1995) 687–694.
 - [35] J.M. Escoubas, M. Lomas, J. Laroche, P.G. Falkowski, Light-intensity regulation of Cab gene-transcription is signaled by the redox state of the plastoquinone pool, *Proc. Natl. Acad. Sci. U. S. A.* 92 (1995) 10237–10241.
 - [36] T.H. Pocock, A. Koziak, D. Rosso, S. Falk, N.P.A. Hüner, *Chlamydomonas raudensis* Etlt.(UWO241), Chlorophyceae, exhibits the capacity for rapid D1 repair in response to chronic photoinhibition at low temperature, *J. Phycol.* (in press).
 - [37] S. Crounman, A. Ruban, P. Horton, PsbS enhances nonphotochemical fluorescence quenching in the absence of zeaxanthin, *FEBS Lett.* 580 (2006) 2053–2058.
 - [38] G. Peltier, L. Cournac, Chlororespiration, *Annu. Rev. Plant Biol.* 53 (2002) 523–550.
 - [39] Y. Munekage, M. Hashimoto, C. Miyake, K. Tomizawa, T. Endo, M. Tasaka, T. Shikanai, Cyclic electron flow around photosystem I is essential for photosynthesis, *Nature* 429 (2004) 579–582.
 - [40] E. Miskiewicz, A.G. Ivanov, N.P.A. Hüner, Stoichiometry of the photosynthetic apparatus and phycobilisome structure of the cyanobacterium *Plectonema boryanum* UTEX 485 are regulated by both light and temperature, *Plant Physiol.* 130 (2002) 1414–1425.
 - [41] Y. Fujita, A study on the dynamic features of photosystem stoichiometry: accomplishments and problems for future studies, *Photosynth. Res.* 53 (1997) 83–93.
 - [42] S. Scherer, Do photosynthetic and respiratory electron transport chains share redox proteins? *Trends Biochem. Sci.* 15 (1990) 458–462.
 - [43] G. Schmetterer, Cyanobacterial respiration, in: D.A. Bryant (Ed.), *The Molecular Biology of Cyanobacteria*, Kluwer Academic Publishers, Dordrecht, 1994, pp. 409–435.
 - [44] M. Hansson, A.V. Vener, Identification of three previously unknown in vivo phosphorylation sites in thylakoid membranes of *Arabidopsis thaliana*, *Mol. Cell Proteomics* 2 (2003) 550–559.

- [45] E. Rintamäki, M. Salonen, U.M. Suoranta, I. Carlberg, B. Andersson, E.M. Aro, Phosphorylation of light-harvesting complex II and photosystem II core proteins shows different irradiance-dependent regulation in vivo. Application of phosphothreonine antibodies to analysis of thylakoid phosphoproteins, *J. Biol. Chem.* 272 (1997) 30476–30482.
- [46] D. Emlyn-Jones, M.K. Ashby, C.W. Mullineaux, A gene required for the regulation of photosynthetic light harvesting in the cyanobacterium *Synechocystis* 6803, *Mol. Microbiol.* 33 (1999) 1050–1058.
- [47] K.S. Siddiqui, R. Cavicchioli, Cold-adapted enzymes, *Annu. Rev. Biochem.* 75 (2006) 403–433.
- [48] G. Feller, C. Gerday, Psychrophilic enzymes: hot topics in cold-adaptation, *Nat. Rev.* 1 (2003) 200–208.